

## Oxygen Isotope Effects upon Reversible O<sub>2</sub>-Binding Reactions: Characterizing Mononuclear Superoxide and Peroxide Structures

Michael P. Lanci and Justine P. Roth\*

Department of Chemistry, Johns Hopkins University, 3400 North Charles Street, Baltimore, Maryland 21218

Received September 26, 2006; E-mail: jproth@jhu.edu

The characterization of intermediates in oxidation reactions of transition metals is a common goal in biological and inorganic chemistry<sup>1</sup> needed to guide the development of new industrial catalysts that can use O<sub>2</sub> as a sacrificial oxidant. Such advances require improved capabilities for identifying metal–O<sub>2</sub> adducts as well as the mechanisms by which these species are formed. In this paper, we examine oxygen equilibrium isotope effects (<sup>18</sup>O EIEs) on reversible reactions that give rise to peroxide (O<sub>2</sub><sup>2-</sup>) and superoxide (O<sub>2</sub><sup>1-</sup>) compounds. The EIEs reported here provide benchmarks for interpreting intermediates during transition-metal-mediated O<sub>2</sub> activation in a variety of natural and synthetic systems.<sup>2–4</sup>

Classic compounds with defined structures (Chart 1)<sup>5</sup> were chosen to examine how <sup>18</sup>O EIEs reflect the reduction of O<sub>2</sub> as well as the mode by which it coordinates to a metal center. The observation of O–O stretching frequencies,  $\nu(\text{O}–\text{O}) = 800–930 \text{ cm}^{-1}$  for side-on peroxide compounds and  $1050–1200 \text{ cm}^{-1}$  for end-on superoxide compounds, has typically served this purpose, although intermediate structures, such as those assigned to side-on superoxide species, have challenged this simple means of classification.<sup>6</sup> In principle, <sup>18</sup>O EIEs complement existing spectroscopic techniques by reporting on changes in O–O bonding together with the formation of new metal–O bonds.

In this work, <sup>18</sup>O EIEs were determined from the oxygen isotope composition of metal–O<sub>2</sub> adducts that had been pre-equilibrated with natural abundance O<sub>2</sub> from air. A detailed description of the high vacuum apparatus and methodology used for preparing samples has been published.<sup>2,3b,7</sup> Samples were analyzed by isotope ratio mass spectrometry (IRMS) which gives <sup>18</sup>O:<sup>16</sup>O to precisions of  $\pm 0.0002$ . The <sup>18</sup>O EIEs were calculated according to eq 1 where  $R_t$  is the <sup>18</sup>O:<sup>16</sup>O in the “total” O<sub>2</sub> isolated from air-saturated solutions containing the metal–O<sub>2</sub> adduct;  $R_u$  is the <sup>18</sup>O:<sup>16</sup>O in the “unbound” O<sub>2</sub> from solutions containing only air and  $1 - f$  is the fraction of metal-bound O<sub>2</sub> in the air-saturated solutions.

$$^{18}\text{O EIE} = \frac{K(^{16}\text{O}^{16}\text{O})}{K(^{18}\text{O}^{16}\text{O})} = \frac{1 - f}{R_t/R_u - f} \quad (1)$$

Reversibility of O<sub>2</sub> binding is a key requirement for accurate and reproducible determinations of <sup>18</sup>O EIEs. Spurious results occur when metal–O<sub>2</sub> adduct decomposition leads to irreversible consumption of O<sub>2</sub> on the time scale of sample collection. In most experiments, the recovery of O<sub>2</sub> was nearly quantitative at  $\geq 22 \text{ }^\circ\text{C}$ ; yields were determined by manometry and based on concentrations of the metal–O<sub>2</sub> adducts detected by multinuclear NMR and UV–vis spectroscopy.<sup>7</sup> Using the same methods, equilibrium constants for O<sub>2</sub> binding ( $K_{\text{O}_2}$ ) under 1 atm of dry air were evaluated as a function of temperature in chlorobenzene (CIBz) or dimethylformamide (DMF) (Table 1).<sup>7</sup>

The metal–O<sub>2</sub> adducts in this study are derived from group IX transition metals. Binding of O<sub>2</sub> to square planar Rh<sup>I</sup> or Ir<sup>I</sup> precursors gives products with side-on peroxide ligands.<sup>8</sup> These structures are characterized by <sup>18</sup>O EIEs of 2–3% in DMF at 22  $^\circ\text{C}$ : 1.0199  $\pm$  0.0017 (Rh), 1.0226  $\pm$  0.0013 (Ir<sub>NCO</sub>), and 1.0305  $\pm$  0.0023 (Ir<sub>Cl</sub>).

Chart 1. Structures and Abbreviations of the Compounds Examined

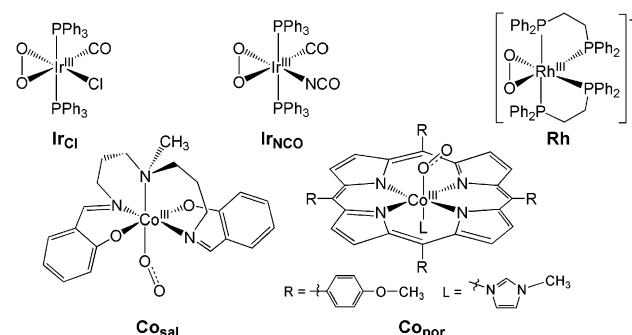


Table 1. Parameters Describing the Reversibility of O<sub>2</sub> Binding

		% yield O <sub>2</sub> <sup>a</sup>	$K_{\text{O}_2} \times 10^{-3}$ (M <sup>-1</sup> ) <sup>a</sup>	$\Delta H^\ddagger$ (kcal mol <sup>-1</sup> )	$\Delta S^\ddagger$ (e.u.)
Ir <sub>Cl</sub>	DMF	82(13)	16(1.9) <sup>b</sup>	-8.4(0.5)	-9.3(3.3)
Ir <sub>NCO</sub>	DMF	93(10)	1.3(0.30)	-7.3(0.5)	-10(2)
Rh	DMF	90(6)	0.47(0.11)	-15.1(0.8)	-37(3)
Co <sub>sal</sub>	DMF	97(5) <sup>c</sup>	0.32(0.02) <sup>c</sup>	-13.1(1.0)	-39(7)
Co <sub>sal</sub>	CIBz	110(19) <sup>d</sup>	0.26(0.05) <sup>d</sup>	-12.4(1.9)	-40(7)
Co <sub>por</sub>	CIBz	94(14) <sup>d</sup>	0.63(0.21) <sup>d</sup>	-8.9(1.0) <sup>f</sup>	-26(4) <sup>f</sup>

<sup>a</sup> Measured at  $22 \pm 2 \text{ }^\circ\text{C}$  under 1 atm of dry air unless noted;  $\pm 1\sigma$  errors are in parentheses. <sup>b</sup> Estimated from  $\Delta H$  and  $\Delta S$  at 22  $^\circ\text{C}$ . <sup>c</sup> At -14  $^\circ\text{C}$ . <sup>d</sup> At -28  $^\circ\text{C}$ . <sup>e</sup> Determined over the following ranges: 40 to 70  $^\circ\text{C}$  (Ir<sub>Cl</sub>), 30 to 60  $^\circ\text{C}$  (Ir<sub>NCO</sub>), 15 to 40  $^\circ\text{C}$  (Rh), 0 to -28  $^\circ\text{C}$  (Co<sub>sal</sub>). <sup>f</sup> From ref 5d with errors  $\pm 2\sigma$ ; determined in toluene from -35 to -80  $^\circ\text{C}$ .

Binding of O<sub>2</sub> to five-coordinate Co<sup>II</sup> precursors gives products with end-on superoxide ligands.<sup>9</sup> Here, lower temperatures were necessary to determine the <sup>18</sup>O EIEs, which are considerably smaller than those quoted above: 1.0041  $\pm$  0.0011 (Co<sub>sal</sub>) in DMF at -14  $^\circ\text{C}$ , 1.0053  $\pm$  0.0017 (Co<sub>sal</sub>) in CIBz at -28  $^\circ\text{C}$ , and 1.0066  $\pm$  0.0013 (Co<sub>por</sub>) in CIBz at -28  $^\circ\text{C}$ . Change in the <sup>18</sup>O EIE for Co<sub>sal</sub> was undetectable from -28 to 0  $^\circ\text{C}$ .<sup>7</sup>

The results for the diverse compounds in solvents of widely varying polarity<sup>10</sup> provide strong evidence that <sup>18</sup>O EIEs are characteristic of the level of O<sub>2</sub> reduction together with the mode by which O<sub>2</sub> binds to the metal (Figure 1). The variation in the observed <sup>18</sup>O EIEs is large considering that the range of calculated <sup>18</sup>O EIEs is 1.00–1.05 for reactions (where O<sub>2</sub> is reduced to HO<sub>2</sub>, H<sub>2</sub>O<sub>2</sub>, H<sub>2</sub>O, O<sub>2</sub><sup>1-</sup>, and O<sub>2</sub><sup>2-</sup>).<sup>11</sup> Further, the distinctive <sup>18</sup>O EIEs for side-on peroxide and end-on superoxide structures are in contrast to the expectation of similar <sup>18</sup>O EIEs ( $\sim 1.01$ ) based on an earlier model.<sup>11</sup> This model assumed analogous bonding within a metal superoxide species and HO<sub>2</sub> as well as within a metal peroxide species and H<sub>2</sub>O<sub>2</sub>.

The formalism of Bigeleisen and Goeppert-Mayer<sup>12</sup> is generally used to calculate heavy atom isotope effects in terms of the change in force constants in proceeding from a reactant to a product state. Using this approach, <sup>18</sup>O EIEs of 1.049 (O<sub>2</sub>  $\rightarrow$  O<sub>2</sub><sup>2-</sup>) and 1.033 (O<sub>2</sub>  $\rightarrow$  O<sub>2</sub><sup>1-</sup>) are predicted for the reduction of O<sub>2</sub> in the absence of concomitant bond formation (Figure 2). Here the size of the <sup>18</sup>O

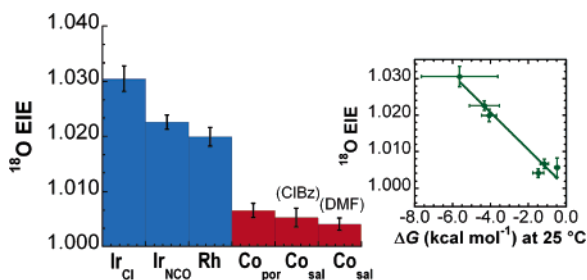


**Figure 1.** Left:  $^{18}\text{O}$  equilibrium isotope effects upon forming the compounds in Chart 1. Right:  $^{18}\text{O}$  EIE versus  $\Delta G$  calculated at 25 °C.

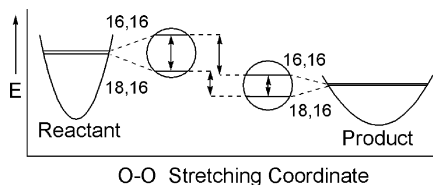


**Figure 2.** Oxygen isotope effect due to a change in O–O force constant; 16,16 and 18,16 designate zero-point energies of the oxygen isotopologues.

EIE is largely determined by the O–O force constant of the product relative to that of  $\text{O}_2$ .<sup>2</sup>

The  $^{18}\text{O}$  EIEs measured for side-on peroxide compounds roughly agree with those calculated using stretching frequencies for the O–O and metal–O normal modes in the above-mentioned approach.<sup>3</sup> We have encountered more difficulty matching the experimental results for  $\text{Co}_{\text{sal}}$  and  $\text{Co}_{\text{por}}$ , where calculated  $^{18}\text{O}$  EIEs are 1.006–1.017. The variations appear to reflect uncertainties in the low-frequency modes.<sup>7</sup> The observed  $^{18}\text{O}$  EIEs are, however, close to values reported for end-on  $\text{Fe}^{\text{III}}$  superoxide species in heme proteins (1.0039–1.0056). In this original work, the small size of the  $^{18}\text{O}$  EIEs was attributed to hydrogen bonding of the terminal oxygen to a nearby amino acid.<sup>11</sup> Such effects are unlikely in the present study since the  $^{18}\text{O}$  EIEs for  $\text{Co}_{\text{sal}}$  and  $\text{Co}_{\text{por}}$  are indistinguishable in DMF and ClBz, yet only DMF has the ability to form hydrogen bonds.

$^{18}\text{O}$  EIEs which characterize the metal– $\text{O}_2$  adducts are likely the result of competing enthalpic and entropic isotope effects,<sup>13</sup> making Figure 2 an oversimplified view. Weakening of the O–O bond contributes to a normal ( $>1$ ) isotope effect upon  $\Delta H$ . Loss of mass-dependent translational and rotational modes when  $\text{O}_2$  coordinates to a metal contributes to a normal isotope effect upon  $\Delta S$ . Offsetting these effects is the formation of new, low-frequency vibrational and rotational modes in the product. The large differences seen for side-on peroxide and end-on superoxide structures suggest that these new modes reduce the  $^{18}\text{O}$  EIEs from the values estimated for  $\text{O}_2^{2-}$  and  $\text{O}_2^{1-}$  yet do not affect the difference due to the change in O–O force constant. This result would seem counterintuitive because the metal–O modes are also expected to influence the  $^{18}\text{O}$  EIE.

The physical origin of  $^{18}\text{O}$  EIEs as well as how they relate to  $^{18}\text{O}$  kinetic isotope effects (KIEs) will be the subject of future investigations. At this stage, some insight may be gleaned from a comparison of the reactions examined here. If it is assumed that the  $^{18}\text{O}$  EIEs for each of the cobalt compounds is the same at 25 °C and the lower experimental temperatures, a trend is observed where the  $^{18}\text{O}$  EIE increases as  $\Delta G$  for  $\text{O}_2$  binding becomes more favorable (Figure 1). The result is in contrast to expectations based upon net bonding changes; the formation of two metal–O bonds stabilizes peroxide compounds relative to superoxide compounds. Instead, the trend seems to indicate that the magnitudes of the  $^{18}\text{O}$  EIEs are largely determined by changes in the O–O force constant, that is, decreases in  $\nu(\text{O}–\text{O})$ . Studies of  $\text{O}_2$  adducts derived from different

metals and having different bonding geometries are currently in progress to further address this interesting observation.

Insofar as  $^{18}\text{O}$  EIEs can be taken as upper limits to  $^{18}\text{O}$  KIEs upon unidirectional  $\text{O}_2$  binding, the present results support previous studies of  $\text{O}_2$  activation by group IX and X metal compounds.<sup>3a</sup> In this work, we reported  $^{18}\text{O}$  KIEs of 1.0069–1.0268 on reactions leading to metal peroxide products. On the grounds that (i) KIEs decreased in proportion to the barriers to  $\text{O}_2$  binding and (ii) no intermediate was detectable in any of the reactions, we proposed a single-step mechanism involving a transition state with peroxide rather than superoxide character. Assuming the above  $^{18}\text{O}$  EIEs as boundary conditions, a KIE  $< 1.007$  would be expected for a transition state leading to a superoxide intermediate and a KIE  $< 1.03$  would be expected for a transition state leading to a peroxide product. Thus, the observed KIEs appear more consistent with a concerted  $2e^-$  mechanism. Of course, a sequential mechanism involving the reorganization of a high-energy superoxide intermediate to a peroxide product in the rate-limiting step cannot be excluded.

In summary, oxygen isotope effects upon reversible  $\text{O}_2$  binding to synthetic transition-metal compounds have been determined for the first time. Using defined systems, we have found that the isotope effect is distinctly different when  $\text{O}_2$  is bound as a side-on peroxide ligand versus an end-on superoxide ligand to a group IX metal. We suggest the ranges of isotope effects for these compounds can serve as benchmarks for identifying transient metal– $\text{O}_2$  adducts. For example, in cases where outer-sphere electron transfer to  $\text{O}_2$  can be ruled out,  $^{18}\text{O}$  KIEs of  $\sim 1\%$  may signal the intermediacy of end-on superoxide species,<sup>2,4</sup> whereas values of 2–3% are consistent with peroxide intermediates. This type of analysis provides a new approach to characterizing intermediates in catalytic oxidation reactions.

**Acknowledgment.** We are grateful for support from NSF CAREER award 0449900 (to J.P.R.) and a Kilpatrick fellowship (to M.P.L.) awarded by the JHU Department of Chemistry.

**Supporting Information Available:** A description of the experiments and calculations. This material is available free of charge via the Internet at <http://pubs.acs.org>.

## References

- (1) (a) *Active Oxygen in Biochemistry*; Valentine, J. S., Foote, C. S., Greenberg, A., Liebman, J. F., Eds.; Chapman & Hall: New York, 1995. (b) *Biomimetic Oxidations Catalyzed by Transition Metal Complexes*; Meunier, B., Ed.; Imperial College Press: London, 2000.
- (2) Roth, J. P.; Klinman, J. P. In *Isotope Effects in Chemistry and Biology*; Kohen, A., Limbach, H. H., Eds.; CRC Press: Boca Raton, FL, 2005.
- (3) Lanci, M. P.; Brinkley, D. W.; Stone, K. L.; Smirnov, V. V.; Roth, J. P. *Angew. Chem., Int. Ed.* **2005**, *44*, 7273. (b) Smirnov, V. V.; Brinkley, D. W.; Lanci, M. P.; Karlin, K. D.; Roth, J. P. *J. Mol. Catal. A* **2006**, *251*, 100.
- (4) (a) Smirnov, V. V.; Roth, J. P. *J. Am. Chem. Soc.* Accepted. (b) Smirnov, V. V.; Roth, J. P. *J. Am. Chem. Soc.* **2006**, *128*, 3683.
- (5) (a) Vaska, L.; Chen, L. S.; Senoff, C. V. *Science* **1971**, *174*, 587. (b) McGinnety, J. A.; Payne, N.; Ibers, J. A. *J. Am. Chem. Soc.* **1969**, *91*, 6301. (c) Trovog, B. S.; Kitko, D. J.; Drago, R. S. *J. Am. Chem. Soc.* **1976**, *98*, 5144. (d) Walker, F. A. *J. Am. Chem. Soc.* **1973**, *95*, 1154.
- (6) Cramer, C. J.; Tolman, W. B.; Theopold, K. H.; Rheingold, A. L. *Proc. Natl. Acad. Sci. U.S.A.* **2003**, *100*, 3635.
- (7) See Supporting Information.
- (8) (a) Vaska, L. *Science* **1963**, *140*, 809. (b) McGinnety, J. A.; Payne, N. C.; Ibers, J. A. *J. Am. Chem. Soc.* **1969**, *91*, 6301. (c) Reed, C. A.; Roper, W. R. *J. Chem. Soc., Dalton Trans.* **1973**, 1370.
- (9) (a) Jones, R. D.; Summerville, D. A.; Basolo, F. *Chem. Rev.* **1979**, *79*, 140. (b) Cini, R.; Orioli, P. *J. Chem. Soc., Dalton Trans.* **1983**, 2564.
- (10) Dielectric constants at 20 °C are  $\epsilon = 36.7$  (DMF) and  $\epsilon = 2.7$  (ClBz); Lide, D. R. *Handbook of Chemistry and Physics*, 74th ed.; CRC Press: Boca Raton, FL, 1993.
- (11) Tian, G.; Klinman, J. P. *J. Am. Chem. Soc.* **1993**, *115*, 8891.
- (12) Bigeleisen, J.; Goepfert-Mayer, M. *J. Chem. Phys.* **1947**, *15*, 26.
- (13) This issue has been discussed extensively for the related reaction of  $\text{H}_2 + \text{IrCl}$ . See: Janak, K. E.; Parkin, G. *J. Am. Chem. Soc.* **2003**, *125*, 13219 and references therein.

JA0669326